



waterscales



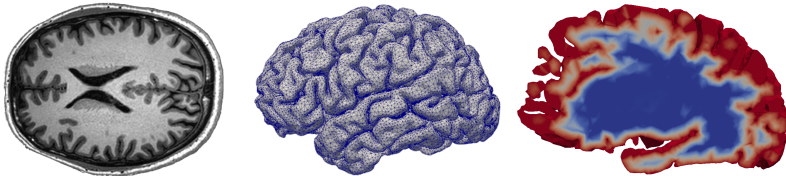
Brain modelling: from magnetic resonance images to finite element simulation

Marie E. Rognes

Oslo, Norway

Jan 15, 22, and 29 2021

Outline of lectures



Lectures 1-2 Quick start: From brain MRI to FEM

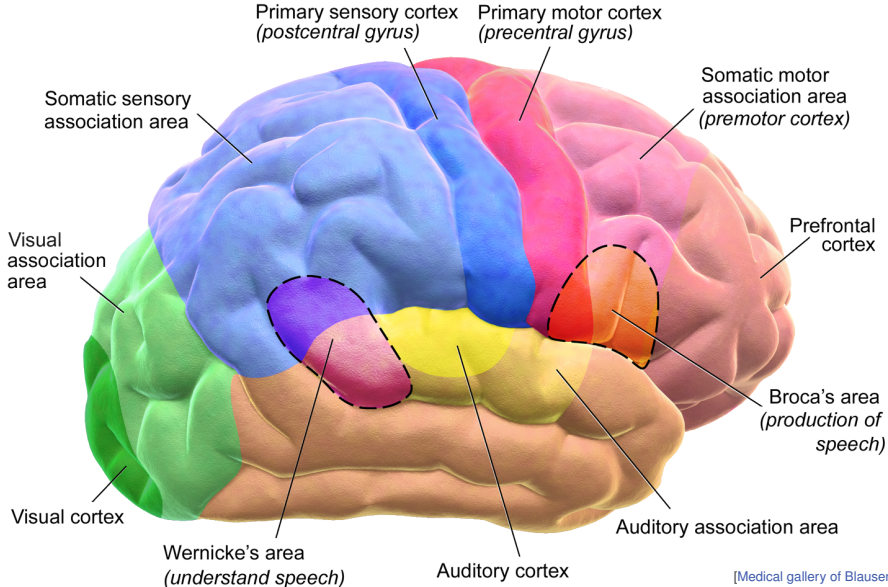
Lectures 3-4 The poroelastic brain

Lectures 5-6 Introducing diffusion tensor images (anisotropy, parcellations)

- I Brain parcellations
- II Anisotropy and the brain
- III Brain physics and chemistry at other scales

I: Brain parcellations

Brain parcellations

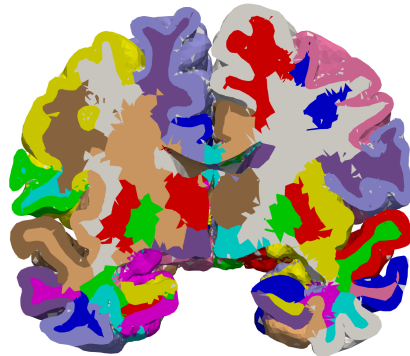


[Medical gallery of Blausen Medical 2014]

The FreeSurfer segmentation process (recon_all) generates volumetric brain parcellations



Parcellation as generated by FreeSurfer and visualized using Freeview.



Same parcellation transferred onto the FEniCS brain mesh and visualized using Paraview.

Converting between voxel space and mesh coordinates

NiBabel is a useful Python module for operating on image data



Parcellation ("wmparc.mgz") in voxel space as generated by FreeSurfer.

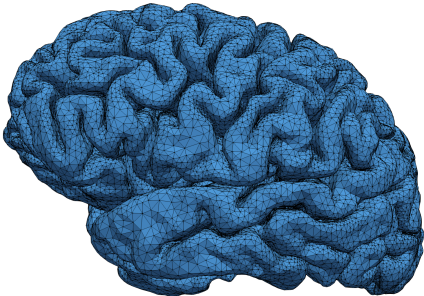
```
import numpy
import nibabel
from nibabel.affines import apply_affine

# Load image, extract its data
# and output its dimensions
image = nibabel.load("wmparc.mgz")
data = image.get_fdata()

# Examine the image dimensions,
# and print some value
print(data.shape)
print(data[100, 100, 100])
```

[<https://nipy.org/nibabel/>]

Representing discrete mesh data in FEniCS

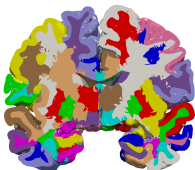
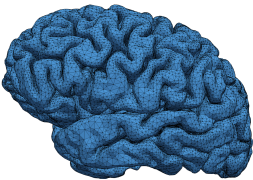


Brain mesh visualized in ParaView.

```
# Import brain mesh
mesh = Mesh()
with XDMFFFile("ernie-brain-32.xdmf") as file:
    file.read(mesh)
print(mesh.num_cells())

# Define cell-based region representation
n = mesh.topology().dim()
regions = MeshFunction("size_t", mesh, n, 0)
print(regions[0])
print(regions.array())
```

Converting brain parcellations between voxel space and RAS



```
# Find the transformation f from T1 voxel space
# to RAS space and take its inverse to get the
# map from RAS to voxel space
vox2ras = image.header.get_vox2ras_tkr()
ras2vox = numpy.linalg.inv(vox2ras)

print("Iterating over all cells...")
for cell in cells(mesh):
    c = cell.index()

    # Extract RAS coordinates of cell midpoint
    xyz = cell.midpoint()[:]

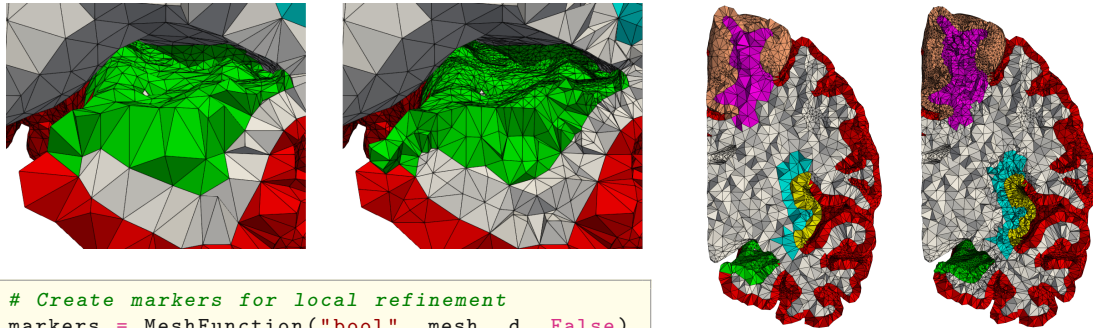
    # Convert to voxel space
    ijk = apply_affine(ras2vox, xyz)

    # Round off to nearest integers to find voxel indices
    i, j, k = numpy.rint(ijk).astype("int")

    # Insert image data into the mesh function:
    regions.array()[c] = int(data[i, j, k])
```

Video example 1: Brain parcellations

Local mesh adaptivity in regions of interest



```
# Create markers for local refinement
markers = MeshFunction("bool", mesh, d, False)

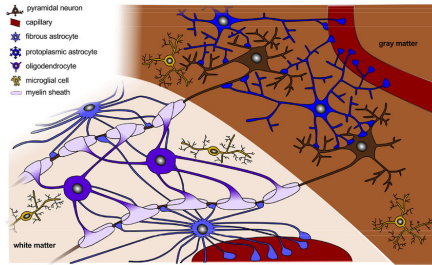
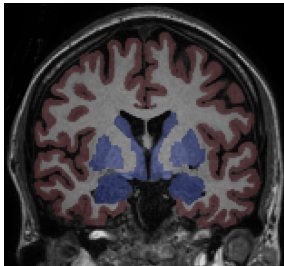
# Iterate over given tags, label all cells
# with this subdomain tag for refinement:
for tag in tags:
    markers.array()[domains.array() == tag] = True

# Refine mesh according to the markers
new_mesh = adapt(mesh, markers)
```

Illustration of left hemisphere meshes with different parcellation regions at different resolutions. The meshes on the right are local refinements of the meshes on the left. Zoomed in view of the hippocampus region (green).

II: Anisotropy in brain characteristics

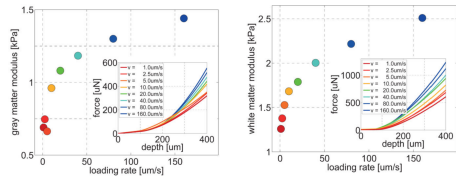
Gray and white matter differs substantially in terms of composition and biophysical properties



Example:

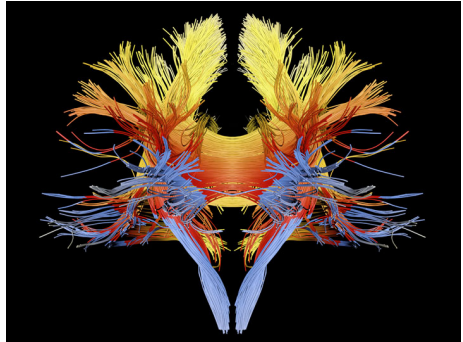
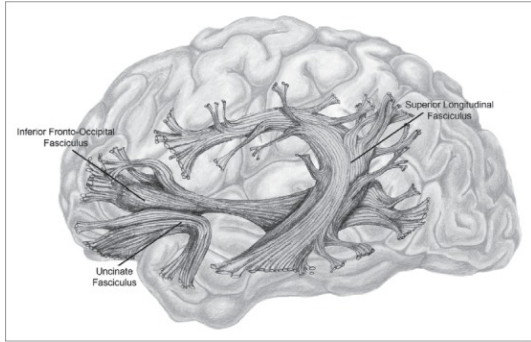
Heterogeneous stiffness (permeability, diffusion) tensor

$$K = K(x) = \begin{cases} K_g & x \in \Omega_g \text{ (in gray matter)}, \\ K_w & x \in \Omega_w \text{ (in white matter)}. \end{cases}$$



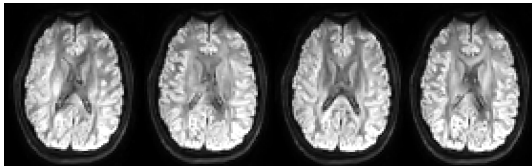
[Budday et al (2015) (Fig 6), Budday et al (2019) (Fig 2)]

White matter fiber tracts induce anisotropy in the brain

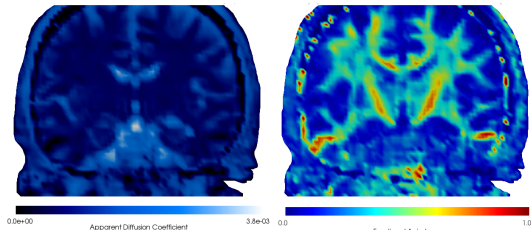


[Left: [Wikimedia Commons](#). Right: Image credit: Alfred Pasieka]

Brain tissue diffusion is anisotropic and can be measured with diffusion tensor imaging



Axial DTI slices measured with different b-vectors. The resolution in the diffusion tensor image is typically lower (here, 96x96x50) compared to that in the T1 images (256x256x256).



Mean diffusivity (left) and fractional anisotropy (right)

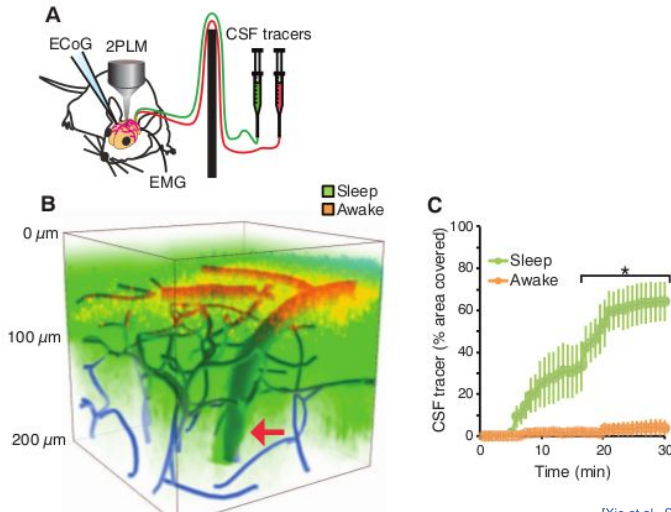
$$D = \begin{pmatrix} d_{11} & d_{12} & d_{13} \\ d_{21} & d_{22} & d_{23} \\ d_{31} & d_{32} & d_{33} \end{pmatrix}, \quad d_{ij} = d_{ij}(x).$$

D sym., pos. def, with eigenpairs (λ_i, v_i) .

$$\text{MD} = \frac{1}{3}(\lambda_1 + \lambda_2 + \lambda_3),$$

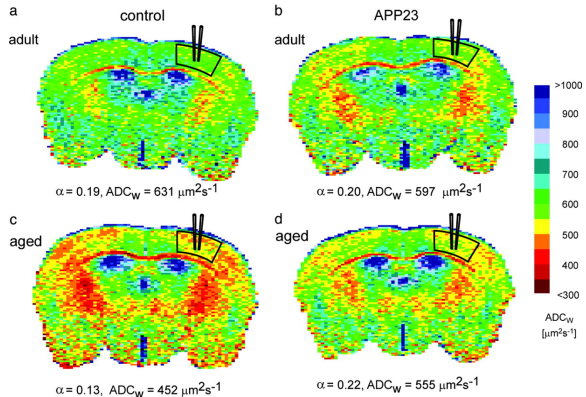
$$\text{FA}^2 = \frac{1}{2} \frac{(\lambda_1 - \lambda_2)^2 + (\lambda_2 - \lambda_3)^2 + (\lambda_3 - \lambda_1)^2}{\lambda_1^2 + \lambda_2^2 + \lambda_3^2}.$$

Tracer experiments in mice indicate an increase in extracellular space volume and more rapid tracer transport during sleep

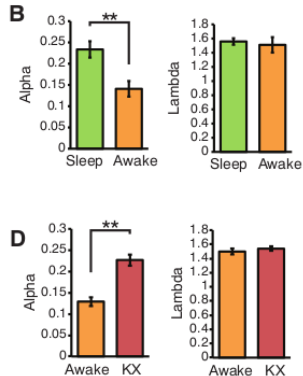


[Xie et al., Science, 2013]

Brain tissue is active and dynamic, and its properties change with circadian rhythm, age and pathologies

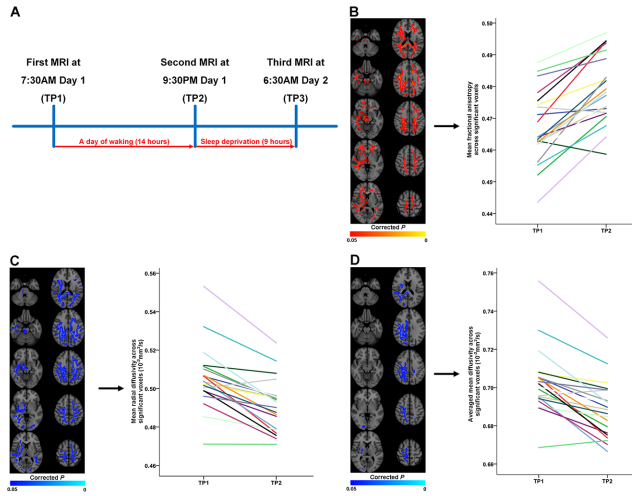


Volume fractions α and apparent diffusion coefficients (ADC) in aging and Alzheimer's disease model mouse (APP23) ([Sykova et al \(2005\)](#) (Fig 2)).



Volume fractions α and tortuosity λ in sleeping, anaesthetized (KX) and awake mice ([Xie et al., Science, 2013](#)).

White matter microstructure changes with sleep and wakefulness: a day of waking gives increased fractional anisotropy



[Elvsåshagen et al (2017) (Fig 1)]

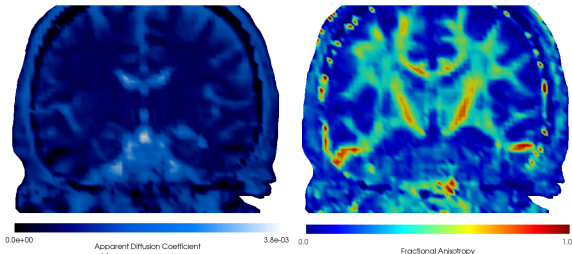
Extracting the diffusion tensor from DTI data using FreeSurfer



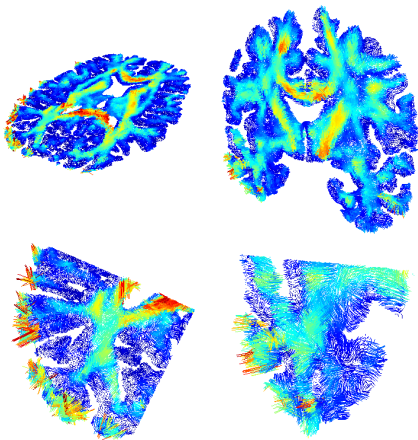
FreeSurfer's `dt_recon` extracts and computes the (per voxel) diffusion tensor, its eigenvalues and eigenvectors, apparent diffusion coefficient/mean diffusivity and fractional anisotropy.

```
$ cd dicom/ernie/DTI  
$ mri_convert IM_0001 dti.mgz
```

```
$ export SUBJECTS_DIR=my-freesurfer-dir  
$ dt_recon --i dti.mgz --b dti.bvals  
dti.voxel_space.bvecs --s ernie --o  
$SUBJECTS_DIR/ernie/dti
```



FEniCS finite element representation of the diffusion tensor



Upper panels show fiber directions (DTI eigenvectors) colored by the fractional anisotropy in the axial and coronal planes. The lower panels show a zoom focusing on the boundary between grey matter and the cerebrospinal fluid.

```
# Read in DTI data in T1 voxel space
dti_image = nibabel.load("tensor.nii")
dti_data = dti_image.get_fdata()
...
ras2vox = numpy.linalg.inv(vox2ras)

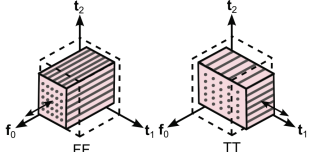
# Create a FEniCS tensor field:
DG9 = TensorFunctionSpace(mesh, "DG", 0)
D = Function(DG9)

# Get dof coordinates
DG0 = FunctionSpace(mesh, "DG", 0)
xyz = DG0.tabulate_dof_coordinates()
...
# Convert to voxel spacen and indices
ijk = apply_affine(ras2vox, xyz).T
i, j, k = numpy.rint(ijk).astype('int')

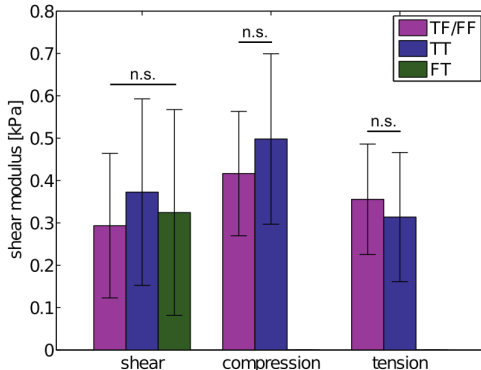
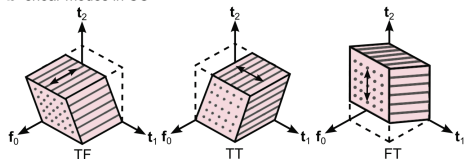
# Create the tensor from the DTI
D1 = dti_data[i, j, k]
D.vector()[:] = D1.reshape(-1)
```

Is brain tissue stiffness notably anisotropic?

a compression/tension modes in CC



b shear modes in CC

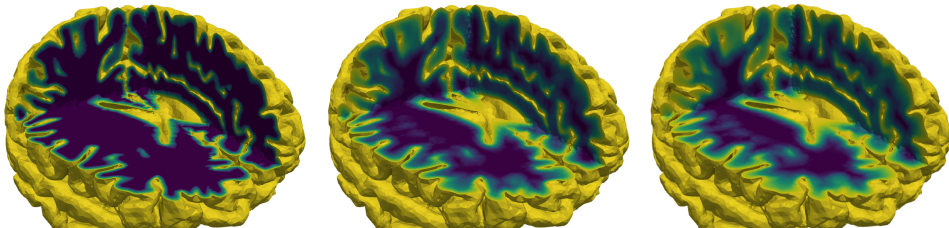
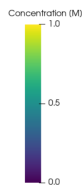
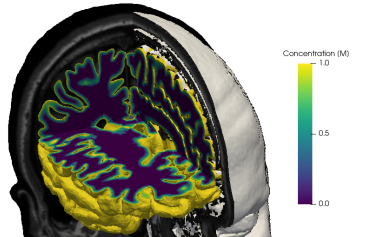


[Budday et al (2017) (Figs 4, 9), 2019]

III: Simulating tracer influx by diffusion in the brain

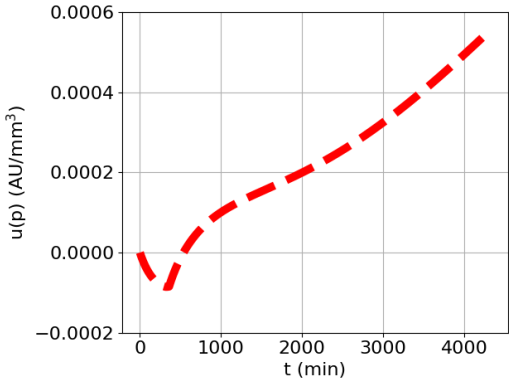
Simulating the distribution of the glymphatic MRI tracer gadobutrol

$$u_t - \operatorname{div} D \operatorname{grad} u = f \text{ in } (0, T] \times \Omega,$$

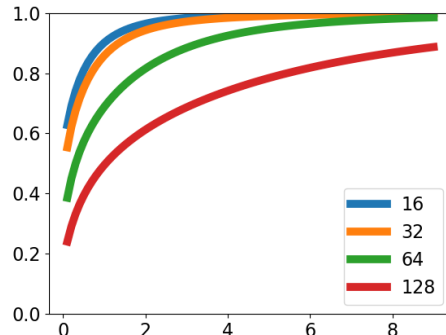
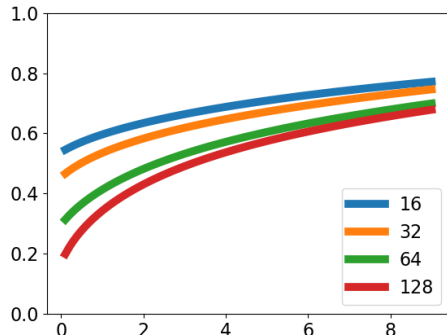


The simulated distribution of gadobutrol after 0 hours (left), after 5 hours (middle) and after 9 hours (right).

Mass lumping

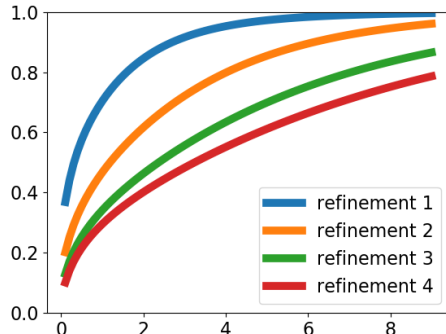
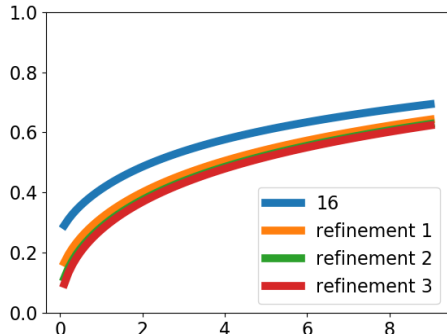


Mass lumping alleviates oscillations at early times at the cost of convergence at later times (I)



Average gadobutrol concentration in the hippocampus (y-axis, arbitrary unit) versus time (x-axis, hours) for different mesh resolutions. Quasi-uniform mesh sequence with $N = 16, 32, 64, 128$ above. Standard Galerkin (left) versus mass-lumped Galerkin (right) discretizations.

Mass lumping alleviates oscillations at early times at the cost of convergence at later times (II)



Average gadobutrol concentration in the hippocampus (y-axis, arbitrary unit) versus time (x-axis, hours) for different mesh resolutions. Adaptively refined mesh sequence. Standard Galerkin (left) versus mass-lumped Galerkin (right) discretizations.

Igor, bring me the last brains!

Want to give it a try? Natural next steps:

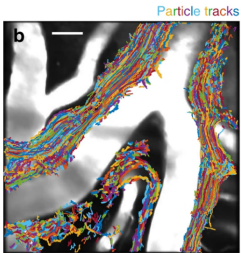
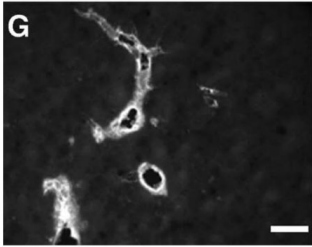
1. Read Chapters 5-6 of [Mardal et al \(2021\)](#)
2. Try out "abby" in the mri2fem data set
3. Explore and have fun!

Brain modelling at other scales

In what sense is perivascular flow driven by arterial pulsations?

[Daversin-Catty et al, PLoS ONE, 2020]

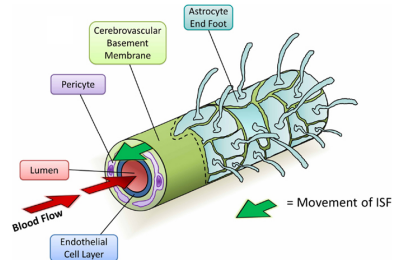
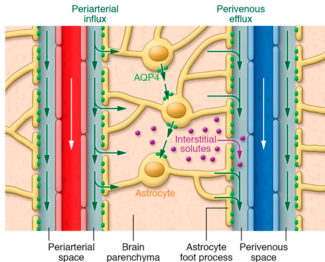
Fluid movement in perivascular spaces enhances solute transport



Key mechanism for brain solute transport: CSF/ISF flow in perivascular spaces – interacting with extra/intracellular water movement.

Open questions Existence? Directionality? Magnitude? Anatomy? Importance?

[Hadaczek et al (2005) (Fig 2), Kaur et al (2020), Iliff et al (2012), Morris et al (2014), Mestre et al (2018) (Fig 1) etc.]



Flow of cerebrospinal fluid through surface perivascular spaces is "driven" by arterial pulsations

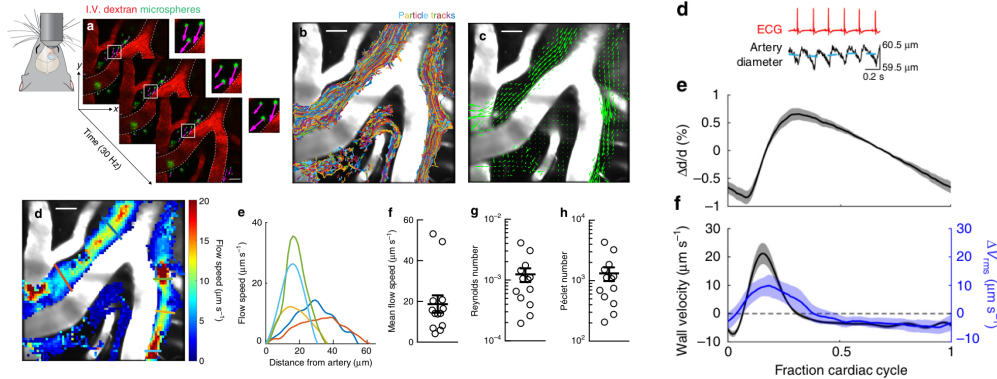
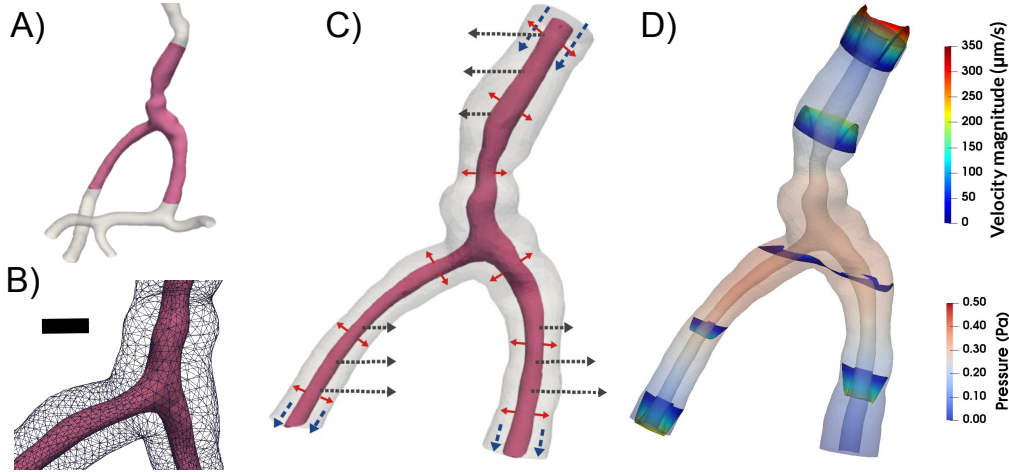


Fig. 1 CSF in the perivascular space is transported via bulk flow. CSF flow was imaged in live mice through a cranial window using two-photon microscopy.

[Mestre et al, Nature Comm., 2018]

To study the mechanisms underlying perivascular flow, we created a computational model from an image-based bifurcating artery



Stokes equations in a perivascular domain with boundary pressures and moving inner boundary

The initial PVS mesh defines the reference domain Ω_0

$X \in \Omega_0 \mapsto \Omega_t \ni x$ with $x = d(X, t)$ for a given deformation d with velocity w .

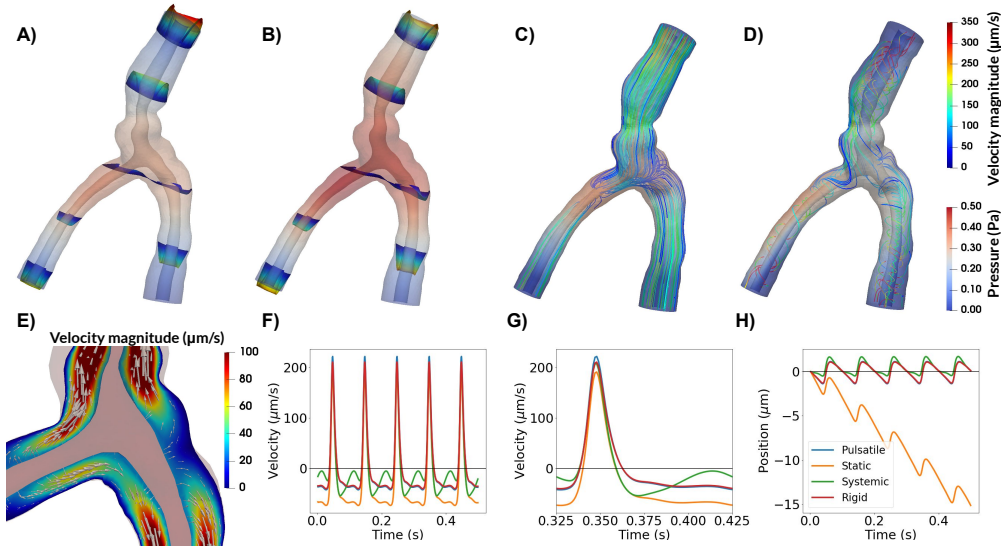
The fluid velocity $v = v(x, t)$ for $x \in \Omega_t$ at time t and the fluid pressure $p = p(x, t)$ then solves [San Martin et al, 2009]:

$$\rho v_t - \mu \nabla^2 v + \nabla p = 0 \quad \text{in } \Omega_t, \tag{1a}$$

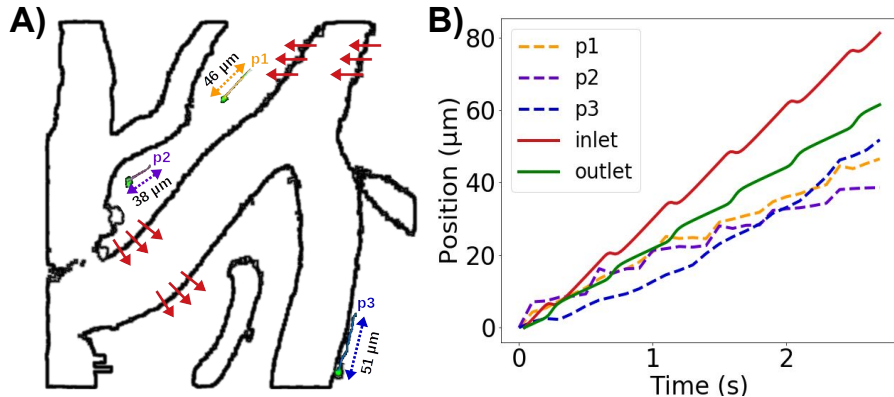
$$\nabla \cdot v = 0 \quad \text{in } \Omega_t. \tag{1b}$$

On the inner PVS wall: $v = w$, outer PVS wall is impermeable and rigid with zero CSF velocity. At the PVS inlet and outlet, we impose given pressures in the form of traction conditions.

Vascular wall pulsations induce oscillatory bi-directional flow patterns in the PVS

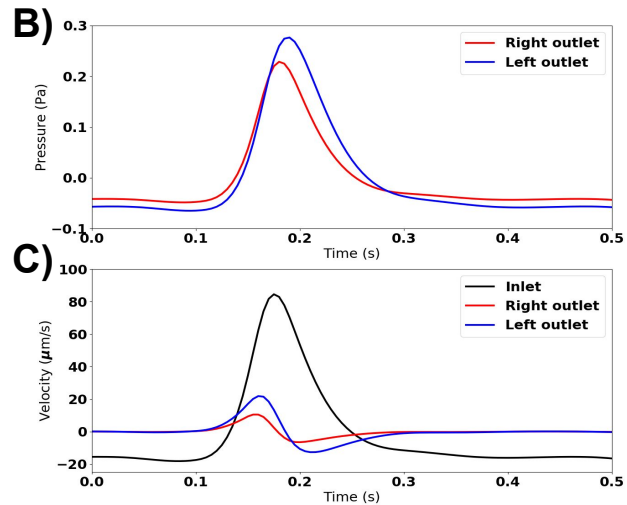
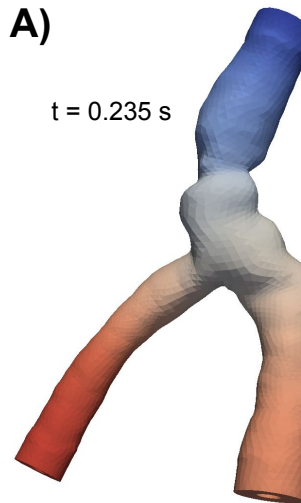


Rigid motions, arterial wall pulsations and a static pressure gradient induced oscillatory PVS flow in agreement with experimental findings

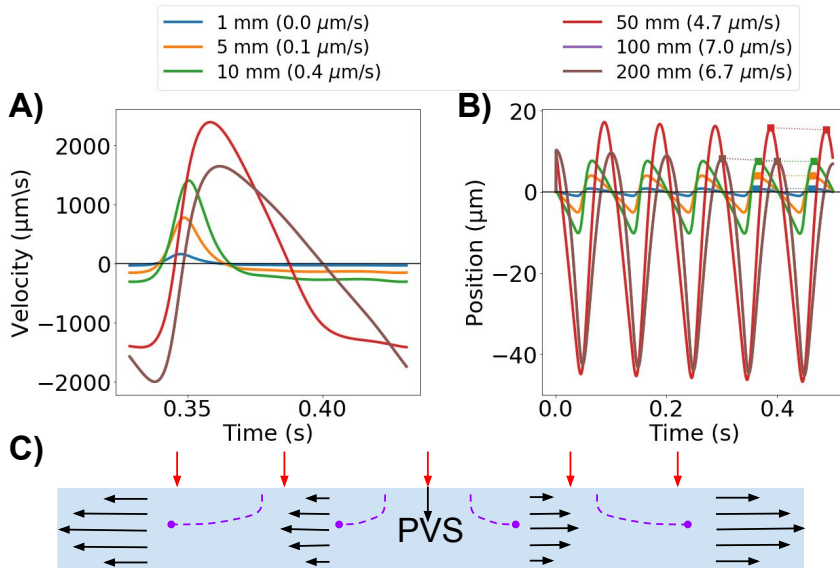


Wall pulsation frequency: 2.2 Hz. Static pressure gradient: 1.46 mmHg.

Compliance and resistance at boundaries change flow characteristics but not net flow



Model length modulates PVS velocity and net flow

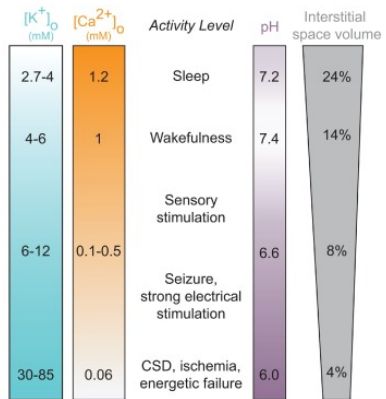


Osmotic versus hydrostatic forces in brain tissue

[Ellingsrud, Dukefoss, Enger, Halnes, Pettersen and Rognes, Validation and knowledge-integration of a computational framework
for ionic electrodiffusion with cortical spreading depression as a case study, in-prep, 2021]

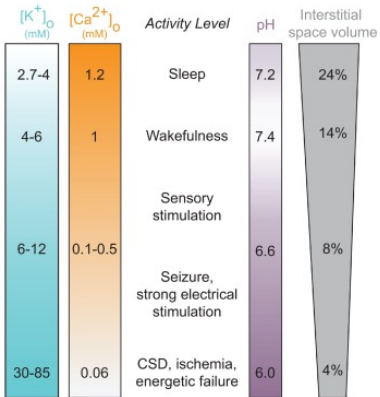
[Ellingsrud, Bouillé, Farrell, and Rognes, Accurate numerical simulation of electrodiffusion and osmotic water movement in brain tissue, in-prep, 2021]

The extracellular ion composition changes with local neuronal activity and across brain states

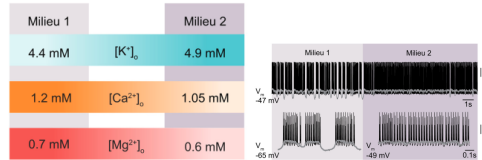


[rasmussen2020interstitial]

The extracellular ion composition changes with local neuronal activity and across brain states

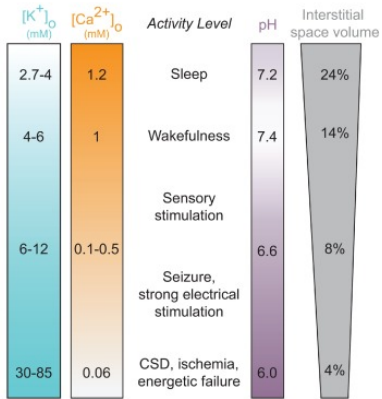


which may affect neuronal activity ...

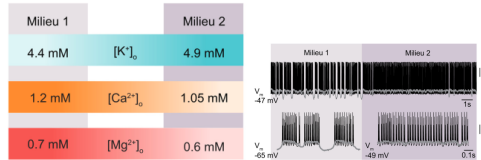


[rasmussen2020interstitial]

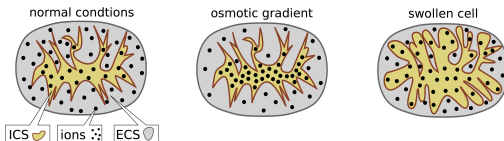
The extracellular ion composition changes with local neuronal activity and across brain states



which may affect neuronal activity ...



... and cause cellular swelling

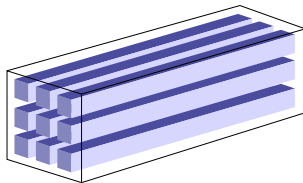


[rasmussen2020interstitial]

Different models of electrodiffusion in brain tissue are suitable for different spatial and temporal scales

KNP-EMI

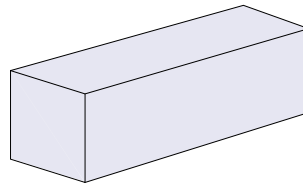
Explicit representation of the cells



cellular (μm)

Model for electrodiffusion and osmosis

Homogenized domain



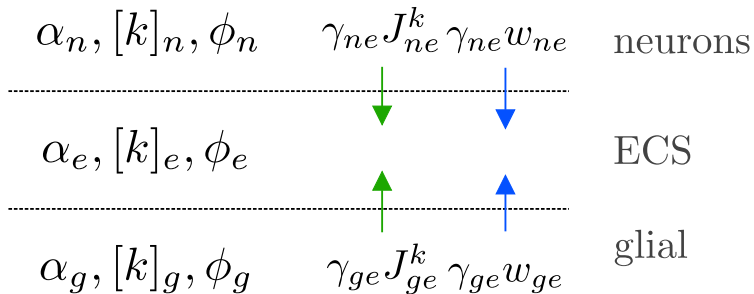
tissue (mm)



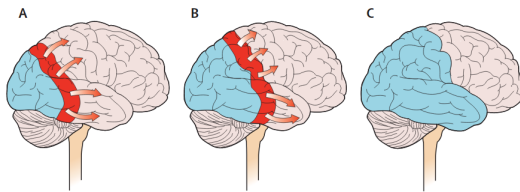
organ (cm)

An homogenized model for ionic electrodiffusion and osmosis

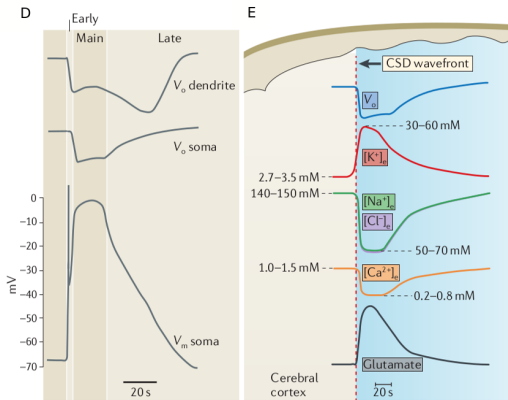
Find the intra-and extracellular volume fractions α_r , the ion concentrations $[k]_r$ and the potentials ϕ_r , for ion species $k \in K$ and compartment $r \in \{n, e, g\}$.



Cortical Spreading Depression (CSD) is a slowly propagating wave of depolarization of brain cells

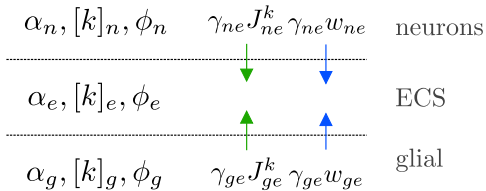


"CSD is a fundamental pattern of brain signaling that provides an opportunity for greater understanding of nervous system physiology..."

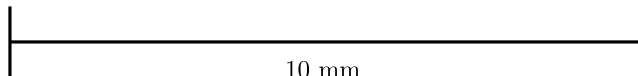
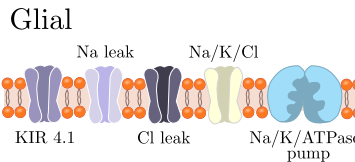
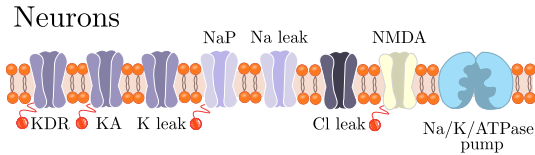


[pietrobon2014chaos]

A mathematical model for ionic electrodiffusion (and fluid movement)

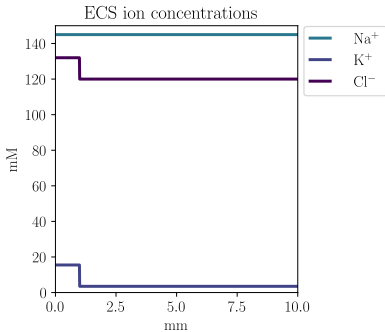
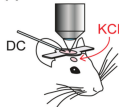


Each compartment contains sodium (Na^+), potassium (K^+), chloride (Cl^-) and glutamate (Glu).



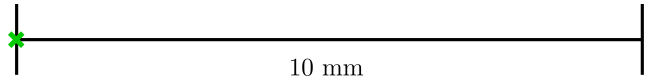
Imitating experimental methods successfully induces model CSD

A



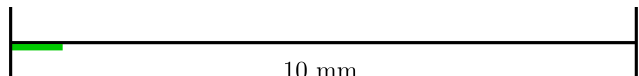
Enger et al (2015). "Dynamics of ionic shifts in cortical spreading depression"

$$I_k = g(\phi_{ne} - E_k), \quad k \in \{\text{Na, K, Cl}\}$$



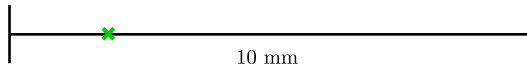
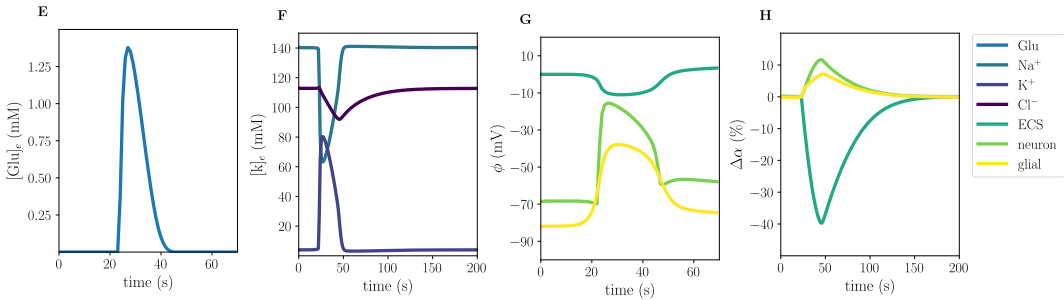
Leao et al (1944). "Spreading depression of activity in the cerebral cortex"

$$I_{\text{pump}} = \frac{I_{\max}}{\left(1 + \frac{m_K}{[K]_e}\right)^2 \left(1 + \frac{m_{\text{Na}}}{[Na]_n}\right)^3}$$



Dreier (2011). "The role of spreading depression, spreading depolarization and spreading ischemia in neurological disease"

Neuron depolarization and breakdown of the ionic homeostasis spreads through the tissue



The Mori framework: volume fractions and osmotic pressure

Find the **volume fractions** $\alpha_r = \alpha_r(\mathbf{x}, t)$ for each compartment $r \in R \cup \{e\}$ (e.g n, g, e) such that:

$$\frac{\partial \alpha_r}{\partial t} = -\gamma_{re} w_{re} \quad r \in R, \tag{2}$$

$$\frac{\partial \alpha_e}{\partial t} = \sum_r \gamma_{re} w_{re}, \tag{3}$$

where:

$$w_{re} = RT\eta_{re} \left(\sum_k ([k]_e - [k]_r) + \frac{a_e}{\alpha_e} - \frac{a_r}{\alpha_r} \right), \tag{4}$$

represents the transmembrane water flux, γ_{re} the area of cell membrane per unit volume, η_{re} the membranes' hydraulic permeability, and a_r the amount of immobile ions.

The Mori framework: ion concentrations and potentials

Further, find the **ion concentrations** $[k]_r = [k]_r(\mathbf{x}, t)$ for all ion species $k \in K$ such that:

$$\frac{\partial(\alpha_r[k]_r)}{\partial t} + \operatorname{div} \mathbf{J}_r^k = -\gamma_{re} J_{re}^k, \quad (5)$$

$$\frac{\partial(\alpha_e[k]_e)}{\partial t} + \operatorname{div} \mathbf{J}_e^k = \sum_{r=1}^{N-1} \gamma_{re} J_{re}^k. \quad (6)$$

We assume that $\frac{\partial \rho_r}{\partial t} = \frac{\partial(\sum_k z_k \alpha_r[k]_r)}{\partial t} = 0$, yielding the following equations for the **potentials** ϕ_r :

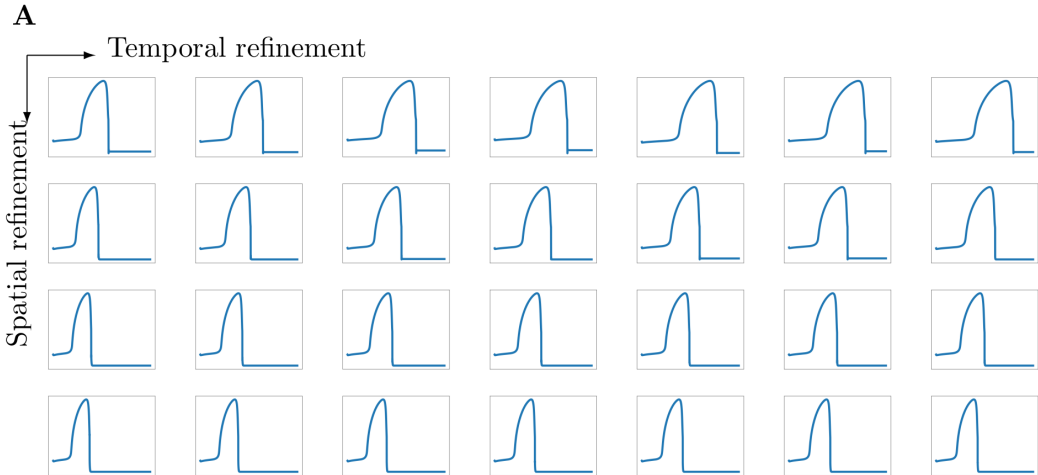
$$F \sum_k z_k \operatorname{div} \mathbf{J}_r^k = -F \sum_k z_k \gamma_{re} J_{re}^k, \quad (7)$$

$$F \sum_k z_k \operatorname{div} \mathbf{J}_e^k = F \sum_k z_k \sum_{r=1}^{N-1} \gamma_{re} J_{re}^k, \quad (8)$$

where J_{re}^k is subject to modelling and:

$$\mathbf{J}_r^k = -D_r^k (\nabla [k]_r + \frac{z_k F}{RT} [k]_r \nabla \phi_r). \quad (9)$$

What is the wave speed of the CSD wave? I



What is the wave speed of the CSD wave? II

B

$N \backslash \Delta t$	12.5	6.25	3.125	1.563	0.781	0.391	0.195	$\Delta \bar{v}_{\text{CSD}}$
1000	7.015	7.923	8.677	9.185	9.477	9.662	9.738	—
2000	5.763	6.385	6.846	7.146	7.331	7.423	7.469	2.269
4000	4.867	5.361	5.716	5.931	6.054	6.123	6.158	1.312
8000	4.688	4.865	5.019	5.147	5.232	5.282	5.305	0.852
$\Delta \bar{v}_{\text{CSD}}$	—	0.178	0.154	0.128	0.085	0.049	0.024	

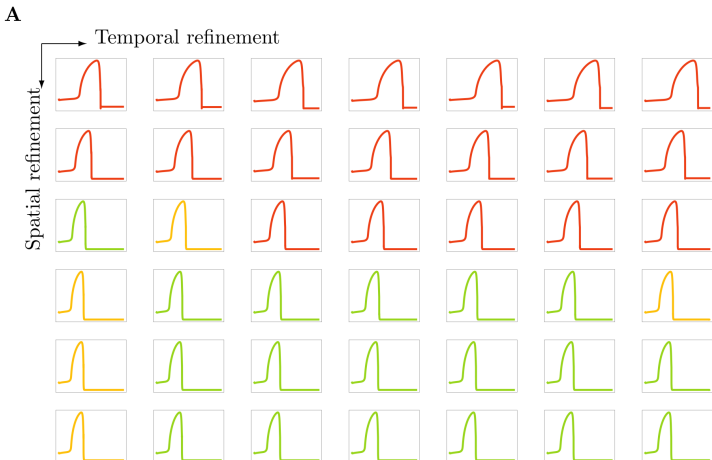
FIG. 1. Wave properties during refinement in space (N) and time (Δt , ms) in a 1D domain of length 10 mm at $t = 50$ s. The PDEs are discretized in time by the previously presented first order scheme from [24, 28, 45] and the ODEs are solved using backward Euler. **A:** Neuron potential $\phi_n(x, 50)$ (mV) versus $x \in \Omega$ (mm). **B:** CSD mean wave speed \bar{v}_{CSD} (mm/min) and difference $\Delta \bar{v}_{\text{CSD}}$ between consecutive refinements.

The wave speed of the CSD wave requires high spatial resolution

Complex system of nonlinear equations

What can numerical investigations of accuracy tell us?

- Splitting scheme (Godunov, Strang)
- Time discretization (BE/CN, ESDIRK/RK...)
- Higher order spatial disc



Giving physiological insight via mathematical modelling

Changes in the glial membrane-surface-area-to-tissue-volume ratio (WT vs WT-B) substantially affects the CSD wave characteristics.

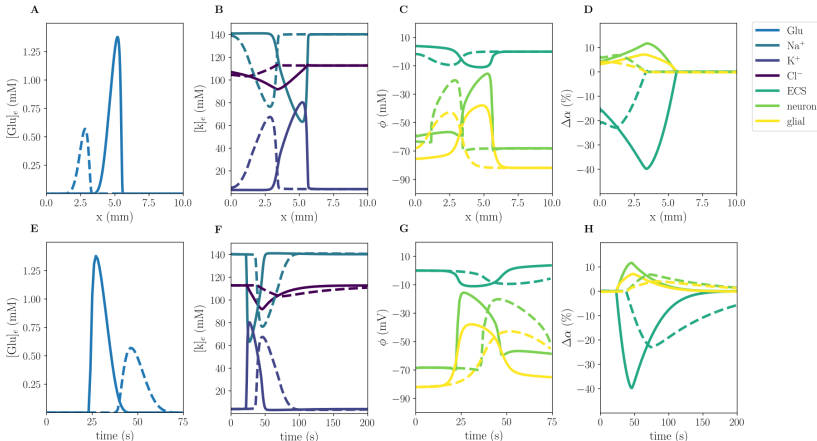


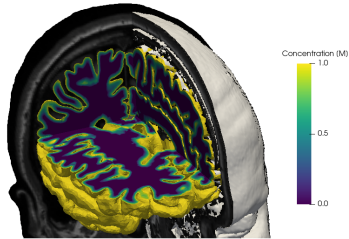
Figure 4. Comparison of WT (solid) and WT-B model (stippled) CSD wave. The upper panels display snapshots of ECS glutamate (**A**), ECS ion concentrations (**B**), potentials (**C**), and change in volume fractions (**D**) at 60 s. The lower panels display time evolution of ECS glutamate (**E**), ECS ion concentrations (**F**), potentials (**G**) and change in volume fractions (**H**) evaluated at $x = 2.0$ mm.

Collaborators

Nicolas Boullé (University of Oxford)
Matteo Croci (University of Oxford)
Cécile Daversin-Catty (Simula Research Laboratory)
Per Kristian Eide (Oslo University Hospital)
Ada Ellingsrud (Simula Research Laboratory)
Rune Enger (University of Oslo)
Patrick E. Farrell (University of Oxford)
Michael B. Giles (University of Oxford)
Jeonghun J. Lee (Baylor University)
Klas Pettersen (University of Oslo)
Eleonora Piersanti (Simula)
Erika K. Lindstrøm (University of Oslo)
Kent-André Mardal (University of Oslo)
Geir Ringstad (Oslo University Hospital)
Travis B. Thompson (University of Oxford)
Lars Magnus Valnes (Simula)
Vegard Vinje (Simula)
... and others

Core message

Mathematical models can give new insight into medicine, – and the human brain gives an extraordinary rich setting for mathematics and numerics!



This research is supported by the European Research Council (ERC) under the European Union's Horizon 2020 research and innovation programme under grant agreement 714892 (Waterscales) by the Research Council of Norway under grant #250731 (Waterscape), and by the EPSRC Centre For Doctoral Training in Industrially Focused 706 Mathematical Modelling (EP/L015803/1).